

## Synthesis and Luminescent Properties of Novel Lanthanide(III) $\beta$ -Diketone Complexes with Nitrogen $p,p'$ -Disubstituted Aromatic Ligands

Anna Bellusci, Giovanna Barberio, Alessandra Crispini,\* Mauro Ghedini, Massimo La Deda, and Daniela Pucci

Centro di Eccellenza CEMIF.CAL-LASCAMM, Unità INSTM della Calabria, Dipartimento di Chimica, 87030 Arcavacata (Cs), Italy

Received August 2, 2004

Tris- $\beta$ -diketonate lanthanide(III) complexes (Ln = Eu, Er, Yb, Tb), of general formula  $[\text{Ln}(\text{acac})_3\text{L}^m]$ , with chelating ligands such as 4,7-disubstituted-1,10-phenanthrolines and 4,4'-disubstituted-2,2'-bipyridines, have been synthesized and fully characterized. The inductive effects of the *para*-substituents on the aromatic N-donor ligands have been investigated both in the solid and in the solution states. Single-crystal X-ray structures have been determined for the diethyl 1,10-phenanthroline-4,7-dicarboxylate europium and 4,4'-dimethoxy-2,2'-bipyridine erbium derivatives, revealing a distorted square antiprismatic geometry around the lanthanide atom in both cases. The influence exerted by the  $p,p'$ -substituents with respect to the nitrogen coordinating atoms on the Ln–N bond distances is discussed comparing the geometrical parameters with those found for the crystal structures containing the fragments  $[\text{Ln}^{\text{III}}(\text{phen})]$  and  $[\text{Ln}^{\text{III}}(\text{bipy})]$  obtained from the Cambridge Structural Database. The influence exerted by the electron-attracting groups on the coordination ability of the ligands, that in some cases becomes lack of coordination of the lanthanide ions, has been also detected in solution where the loss of the ligand has been followed by UV–vis spectroscopy. Moreover, the use of relatively long alkoxy chains as substituents on the 1,10-phenanthroline ligand led to the formation of a promesogenic lanthanide complex, whose thermal behavior is encouraging for the synthesis of new lanthanide liquid-crystalline species.

### Introduction

The unique physical properties of lanthanide ions are the main reason lanthanide complexes are of great importance in industrial, chemical, medical, and sensor applications.<sup>1,2</sup> Several of the lanthanide (Ln) ions show very intense luminescence characterized by very narrow emission bands, a long decay time, and a large difference between the excitation and emission wavelengths, a property that can be used to decrease the interference caused by background and scattering.<sup>3</sup> They are therefore increasingly used as highly efficient electroluminescent components for light-emitting diodes,<sup>4–6</sup> luminescence probes for analytes,<sup>7,8</sup> labels for

proteins and amino acids,<sup>9</sup> and for molecular recognition and chirality sensing of biological substrates.<sup>10</sup> Moreover, by incorporating lanthanide ions into liquid crystals, it is possible to obtain luminescent and mesogenic complexes that are useful for the design of emissive liquid crystal displays and magnetically addressable liquid crystals.<sup>11</sup>

The optical properties of the lanthanide cations are different from other metal ions and molecular species because they absorb and emit light over narrow wavelength ranges.

\* Author to whom correspondence should be addressed. E-mail: a.crispini@unical.it.

- (1) Bünzli, G. J.-C.; Piguet, C. *Chem. Rev.* **2002**, *102*, 1897–1928.
- (2) Tsukube, H.; Shinoda, S. *Chem. Rev.* **2002**, *102*, 2389–2403.
- (3) Mukkala, V.-M.; Sund, C.; Kwiatkowski, M.; Pasanen, P.; Hogberg, M.; Kankare, J.; Takalo, H. *Helv. Chim. Acta* **1992**, *75*, 1621–1632.
- (4) Curry, R. J.; Gillin, W. P. *Curr. Opin. Solid State Mater. Sci.* **2001**, *5*, 481–486.

- (5) Capecchi, S.; Renault, O.; Moon, D.-G.; Halim, M.; Etchells, M.; Dobson, P. J.; Salata, O. V.; Christou, V. *Adv. Mater.* **2000**, *12*, 1591–1594.
- (6) Kido, J.; Okamoto, Y. *Chem. Rev.* **2002**, *102*, 2357–2368.
- (7) Parker, D. *Coord. Chem. Rev.* **2000**, *205*, 109–130.
- (8) Elbanowski, M.; Makowska, B. J. *Photochem. Photobiol., A: Chem.* **1996**, *99*, 85–92.
- (9) Yam, V. W. W.; Lo, K. K. W. *Coord. Chem. Rev.* **1999**, *184*, 157–240.
- (10) Tsukube, H.; Shinoda, S.; Tamiaki, H. *Coord. Chem. Rev.* **2002**, *226*, 227–234.
- (11) Binnemans, K.; Görrler-Walrand, C. *Chem. Rev.* **2002**, *102*, 2303–2354.

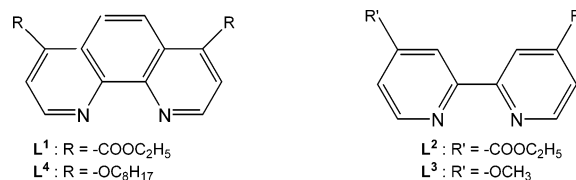
Unfortunately, the lanthanide ions are characterized by a very low absorption coefficient ( $\epsilon < 1 \text{ M}^{-1} \text{ cm}^{-1}$ ), which makes direct excitation of the emitting levels impossible. Furthermore, coordination of solvent molecules to the lanthanide ions has dramatic effects on their excited state decay, because this decay is mainly governed by nonradiative process. When solvents containing O–H groups are coordinated to lanthanide ions, efficient nonradiative deactivations take place via vibronic coupling with the vibrational states of the O–H oscillators.<sup>12</sup>

A way to circumvent these difficulties is to use ligands bearing suitable chromophores capable of forming, with Ln(III) ions, thermodynamically stable complexes; these ligands could play the antenna role, absorbing light and transferring excitation energy to the emitting ion. Additionally, when the Ln<sup>3+</sup> cation is coordinatively unsaturated by the original ligands, an additional neutral ligand coordinates with the lanthanide center to form a highly coordinated complex thereby excluding the coordination of solvent molecules. Representative examples of the formation of highly coordinated complexes are the lanthanide tris( $\beta$ -diketonates) containing several nitrogen ligands such as 2,2'-bipyridine,<sup>13</sup> 1,10-phenanthroline,<sup>14</sup> and 2,2':6',6''-terpyridine.<sup>15,16</sup> The interaction between lanthanide ions and these organic ligands and the formation of new complexes with increased coordination number has the effect of protecting metal ions from vibrational coupling and increasing their light absorption cross section by the "antenna effect".

While it is well known that europium(III) and terbium(III)- $\beta$ -diketone complexes are efficient labels for immunoassays, their derivatives with 2,2'-bipyridine and 1,10-phenanthroline promise extensive photophysical applications.<sup>17</sup>

As part of our continuing research exploring the potential for forming luminescent and liquid-crystalline complexes containing 4,4'-disubstituted 2,2'-bipyridine ligands,<sup>18,19</sup> we have attempted the synthesis of Ln(III) complexes (Ln = Eu, Er, Yb, Tb) with similar disubstituted aromatic N-donor ligands containing various substituents in *p,p'*-positions with respect to the coordinating nitrogen atoms. Tris- $\beta$ -diketonate lanthanide complexes with 2,2'-bipyridine and 1,10-phenanthroline were first reported several years ago,<sup>20</sup> and an interesting study of the influence of electron-withdrawing groups of the  $\beta$ -diketonate ligands on the coordination

Chart 1



number of the lanthanide ions in similar systems has been recently reported.<sup>21</sup> Moreover, the use of suitable substituents on the  $\beta$ -diketonate ligands has been shown to induce liquid-crystalline behavior in lanthanide complexes where the Lewis base is either 1,10-phenanthroline, 2,2'-bipyridine, or an alkanoyloxy 5,5'-disubstituted 2,2'-bipyridine.<sup>22</sup>

The goal of our work is to determine whether the electronic effect of the *para*-substituents of the aromatic N-donor ligands (4,7-disubstituted 1,10-phenanthrolines and 4,4'-disubstituted 2,2'-bipyridines, Chart 1) would be reflected in the structure as well as in the physical properties of simple tris-acetylacetonate lanthanide(III) complexes. Therefore, new Ln acetylacetonate complexes containing variously substituted N,N aromatic ligands,  $L^m$ , have been synthesized, and two of them, the [Eu(acac)<sub>3</sub>L<sup>1</sup>], **1**, and [Er(acac)<sub>3</sub>L<sup>3</sup>], **7**, have been structurally characterized. Photophysical properties are also reported. Moreover, the use of relatively long alkoxy chains as substituents on the 1,10-phenanthroline ligand ( $L^4$ ) leads to the formation of the promesogenic lanthanide complex, **9**, whose thermal behavior is promising for the synthesis of Ln derivatives in which the mesomorphism is introduced via an appropriately substituted N,N aromatic ligand.

## Experimental Section

**General.** The commercially available chemicals that were used without further purification follow: europium(III) nitrate pentahydrate 99.9% (Aldrich); terbium(III) nitrate pentahydrate 99.9% (Aldrich); erbium(III) nitrate pentahydrate 99.9% (Aldrich); ytterbium(III) nitrate pentahydrate 99.9% (Aldrich); acetylacetonate 99% (Aldrich); 4,7-dimethyl-1,10-phenanthroline 98% (Aldrich); 4,7-dihydroxy-1,10-phenanthroline 99% (Aldrich); 1-bromooctane 99% (Aldrich); and 4,4'-dimethoxy-2,2'-bipyridine ( $L^3$ ) 97% (Acros Organics).

The <sup>1</sup>H NMR spectra were recorded on a Bruker WH-300 spectrometer in CDCl<sub>3</sub> solution, with TMS as internal standard. Elemental analyses were performed with a Perkin-Elmer 2400 microanalyzer by the Microanalytical Laboratory at the University of Calabria. 4,7-Dicarboxy-1,10-phenanthroline,<sup>23</sup> 4,4'-dicarboxy-2,2'-bipyridine,<sup>19</sup> and lanthanide acetylacetonates<sup>24</sup> were prepared according to the literature procedures.

**Synthesis of Diethyl 1,10-Phenanthroline-4,7-dicarboxylate, L<sup>1</sup>.** One milliliter of sulfurous acid was added to a solution of 4,7-dicarboxy-1,10-phenanthroline (0.250 g, 0.93 mmol) dissolved in

- (12) Sabbatini, N.; Guardigli, M.; Lehn, J.-M. *Coord. Chem. Rev.* **1993**, *123*, 201–228.
- (13) Bekiari, V.; Lianos, P. *Adv. Mater.* **1998**, *10*, 1455–1458.
- (14) Christidis, P. C.; Tossidis, I. O.; Paschalidis, D. G.; Tzavellas, L. C. *Acta Crystallogr.* **1998**, *C54*, 1233–1236.
- (15) Fukuda, Y.; Nakao, A.; Hayashi, K. *J. Chem. Soc., Dalton Trans.* **2002**, 527–533.
- (16) Cotton, S. A.; Noy, O. E.; Liesener, F.; Raithby, P. R. *Inorg. Chim. Acta* **2003**, *344*, 37–42.
- (17) Guan, M.; Bian, Z. Q.; Li, F. Y.; Xin, H.; Huang, C. H. *New J. Chem.* **2003**, 27, 1731–1734.
- (18) (a) Pucci, D.; Barberio, G.; Crispini, A.; Francescangeli, O.; Ghedini, M.; La Deda, M. *Eur. J. Inorg. Chem.* **2003**, 3649–3661. (b) Barberio, G.; Bellusci, A.; Crispini, A.; Ghedini, M.; Golemme, A.; Prus, P.; Pucci, D. *Eur. J. Inorg. Chem.* **2005**, 181–188.
- (19) Pucci, D.; Barberio, G.; Crispini, A.; Francescangeli, O.; Ghedini, M. *Mol. Cryst. Liq. Cryst.* **2003**, *395*, 325–335.
- (20) Watson, W. H.; Williams, R. J.; Stemple, N. R. *J. Inorg. Nucl. Chem.* **1972**, *34*, 501–508.

- (21) van Staveren, D. R.; van Albada, G. A.; Haasnoot, J. G.; Kooijman, H.; Manotti Lanfredi, A. M.; Nieuwenhuizen, P. J.; Spek, A. L.; Ugozzoli, F.; Weyhermüller, T. Reedijk, J. *Inorg. Chim. Acta* **2001**, *315*, 163–171.
- (22) Galyametdinov, Yu. G.; Malykhina, L. V.; Haase, W.; Driesen, K.; Binnemans, K. *Liq. Cryst.* **2002**, *29*, 1581–1584.
- (23) Yanagida, M.; Singh, P. L.; Sayama, K.; Hara, K.; Katoh, R.; Islam, A.; Sugihara, H.; Arakawa, H.; Nazeeruddin, M. K.; Grätzel, M. *J. Chem. Soc., Dalton Trans.* **2000**, 2817–2822.
- (24) Fernelius, W. C. *Inorg. Synth.* **1946**, *2*, 123–125.

60 mL of ethanol. The yellow reaction mixture was refluxed for 5 days, and then it was allowed to cool to room temperature. The solvent was evaporated, and chloroform (35 mL) was added. The resultant mixture was washed with saturated  $\text{Na}_2\text{CO}_3$  solution ( $2 \times 35$  mL) and then with water (30 mL). The organic extract was dried ( $\text{Na}_2\text{SO}_4$ ), filtered, and evaporated. The product was recrystallized from hexane, to give **L**<sup>1</sup> as a brown solid (0.196 g, 65%). mp 167 °C. Anal. Calcd for  $\text{C}_{18}\text{H}_{16}\text{N}_2\text{O}_4$ : C, 66.26; H, 4.97; N, 8.64. Found: C, 65.83; H, 5.20; N, 8.38. <sup>1</sup>H NMR ( $\text{CDCl}_3$ ):  $\delta$  9.31 (d, <sup>2</sup>*J* = 4.4 Hz, 2H, H<sup>2,9</sup>);  $\delta$  8.88 (s, 2H, H<sup>5,6</sup>);  $\delta$  8.14 (d, <sup>2</sup>*J* = 4.4 Hz, 2H, H<sup>3,8</sup>);  $\delta$  4.54 (m, 4H, OCH<sub>2</sub>);  $\delta$  1.50 (t, 6H, CH<sub>3</sub>).

**Synthesis of Diethyl 2,2'-Bipyridine-dicarboxylate, L**<sup>2</sup>. 4,4'-Dicarboxy-2,2'-bipyridine (0.24 g, 0.98 mmol) was refluxed with sulfuric acid (95–97%, 0.6 mL) in absolute ethanol (10 mL) until total solubilization. After 24 h, the solution was evaporated to dryness and the crude product, suspended in water, was extracted with chloroform ( $3 \times 50$  mL). Recrystallization from chloroform/methanol led to the pure product as white powder (0.290 g, 83%). mp 157 °C. Anal. Calcd for  $\text{C}_{16}\text{H}_{16}\text{N}_2\text{O}_4$ : C, 63.99; H, 5.37; N, 9.33. Found: C, 63.98; H, 5.15; N, 9.64. <sup>1</sup>H NMR ( $\text{CDCl}_3$ ):  $\delta$  8.95 (s, 2H; H<sup>3,3'</sup>);  $\delta$  8.87 (d, <sup>3</sup>*J* = 5.0 Hz, 2H; H<sup>6,6'</sup>);  $\delta$  7.91 (dd, <sup>3</sup>*J* = 5.0 Hz, <sup>4</sup>*J* = 1.5 Hz, 2H; H<sup>5,5'</sup>);  $\delta$  4.46 (q, <sup>3</sup>*J* = 7.0 Hz, 4H; CH<sub>2</sub>);  $\delta$  1.45 (t, <sup>3</sup>*J* = 7.0 Hz, 6H; CH<sub>3</sub>).

**Synthesis of 4,7-Dioctyloxy-1,10-phenanthroline, L**<sup>4</sup>. To a suspension of 4,7-dihydroxy-1,10-phenanthroline (0.200 g, 0.94 mmol) in 15 mL of DMSO was added KOH (0.106 g, 1.88 mmol), and the slurry was stirred at room temperature for 2 days. Next, 1-bromooctane (0.857 g, 4.44 mmol) was placed in the flask. The reaction mixture was stirred at room temperature for 4 days, and then poured into water (10 mL) and extracted with ethyl acetate ( $3 \times 20$  mL). The ethyl acetate extracts were combined and washed repeatedly with water ( $3 \times 15$  mL) and then with an aqueous basic solution (5% NaOH). The organic phase was shaken with a saturated aqueous NaCl solution, dried over magnesium sulfate, and evaporated under vacuum. The crude product was further purified by chromatography (silica gel,  $\text{CHCl}_3$ ; *R*<sub>f</sub> = 0). **L**<sup>4</sup> was recrystallized by MeOH and obtained as a brown solid (0.061 g, 15%). mp 103 °C. Anal. Calcd for  $\text{C}_{28}\text{H}_{40}\text{N}_2\text{O}_2$ : C, 77.02; H, 9.23; N, 6.42. Found: C, 76.90; H, 9.35; N, 6.24. <sup>1</sup>H NMR ( $\text{CDCl}_3$ ):  $\delta$  8.91 (d, <sup>2</sup>*J* = 5.1 Hz, 2H, H<sup>2,9</sup>);  $\delta$  8.12 (s, 2H, H<sup>5,6</sup>);  $\delta$  6.89 (d, <sup>2</sup>*J* = 5.1 Hz, 2H, H<sup>3,8</sup>);  $\delta$  4.16 (t, 4H, OCH<sub>2</sub>);  $\delta$  1.55 (m, 24H, CH<sub>2</sub>);  $\delta$  1.17–1.1 (t, 6H, CH<sub>3</sub>).

**Synthesis of [Ln(acac)<sub>3</sub>L<sup>m</sup>]**. Ln(acac)<sub>3</sub> (0.492 mmol) and the stoichiometric amount of the ligand were dissolved in 30 mL of toluene. The solution was stirred for 15 days at room temperature and then evaporated to dryness. The residue was crystallized from chloroform/hexane to give the pure product.

All homologues were synthesized by the same method described above. Yields, color, elemental analyses, and melting temperatures are as follows.

**[Eu(acac)<sub>3</sub>L<sup>1</sup>]**, **1**. (0.278 g, 73%); yellow solid. Anal. Calcd for  $\text{C}_{33}\text{H}_{37}\text{N}_2\text{O}_{10}\text{Eu}$ : C, 51.23; H, 4.82; N, 3.62. Found: C, 51.69; H, 5.00; N, 3.24. mp 240 °C (dec).

**[Tb(acac)<sub>3</sub>L<sup>1</sup>]**, **2**. (0.292 g, 76%); yellow solid. Anal. Calcd for  $\text{C}_{33}\text{H}_{37}\text{N}_2\text{O}_{10}\text{Tb}$ : C, 50.78; H, 4.78; N, 3.59. Found: C, 50.88; H, 4.59; N, 3.22. mp 230 °C.

**[Er(acac)<sub>3</sub>L<sup>1</sup>]**, **3**. (0.307 g, 79%); yellow solid. Anal. Calcd for  $\text{C}_{33}\text{H}_{37}\text{N}_2\text{O}_{10}\text{Er}$ : C, 50.24; H, 4.73; N, 3.55. Found: C, 49.94; H, 4.62; N, 3.98. mp 216 °C.

**[Yb(acac)<sub>3</sub>L<sup>1</sup>]**, **4**. (0.317 g, 81%); yellow solid. Anal. Calcd for  $\text{C}_{33}\text{H}_{37}\text{N}_2\text{O}_{10}\text{Yb}$ : C, 49.88; H, 4.69; N, 3.52. Found: C, 50.20; H, 4.42; N, 4.08. mp 267 °C.

**Table 1.** Crystallographic Data for Complexes **1** and **7**

	<b>1</b>	<b>7</b>
empirical formula	$\text{C}_{33}\text{H}_{37}\text{N}_2\text{O}_{10}\text{Eu}$	$\text{C}_{27}\text{H}_{36}\text{N}_2\text{O}_8\text{Er}$
fw	773.61	683.84
cryst syst	monoclinic	monoclinic
space group	<i>C2/c</i>	<i>P2<sub>1</sub></i>
<i>a</i> , Å	15.303(3)	8.641(1)
<i>b</i> , Å	28.546(6)	16.578(2)
<i>c</i> , Å	16.856(3)	10.164(1)
$\beta$ , deg	110.89(3)	96.79(2)
<i>V</i> , Å <sup>3</sup>	6879(2)	1445.8(3)
<i>Z</i>	8	2
<i>D</i> (calcd), g/cm <sup>3</sup>	1.494	1.571
$\mu$ , mm <sup>-1</sup>	1.880	2.951
temp, K	298	298
<i>F</i> (000)	3136	688
$\theta$ (deg)	1.59–26.06	2.02–28.44
no. measured reflns	7067	11 520
no. unique reflns	6805 [ <i>R</i> (int) = 0.0512]	6310 [ <i>R</i> (int) = 0.0135]
reflns with <i>I</i> > 2 $\sigma$ ( <i>I</i> )	3739	5677
refined params	416	338
GOF	0.936	1.15
<i>R</i> indices <sup>a,b</sup>	<i>R</i> 1 = 0.0668, <i>wR</i> 2 = 0.1330	<i>R</i> 1 = 0.0269, <i>wR</i> 2 = 0.0734
<i>R</i> indices (all data)	<i>R</i> 1 = 0.1268, <i>wR</i> 2 = 0.1576	<i>R</i> 1 = 0.0316, <i>wR</i> 2 = 0.0797

$$^a R1 = \sum(|F_o| - |F_c|) / \sum|F_o|. \quad ^b wR2 = [\sum w(F_o^2 - F_c^2)^2 / \sum w(F_o^2)^2]^{1/2}.$$

**[Eu(acac)<sub>3</sub>L<sup>3</sup>]**, **5**. (0.278 g, 85%); white solid. Anal. Calcd for  $\text{C}_{27}\text{H}_{33}\text{N}_2\text{O}_8\text{Eu}$ : C, 48.73; H, 5.00; N, 4.21. Found: C, 50.11; H, 5.00; N, 4.63. mp 263 °C (dec).

**[Tb(acac)<sub>3</sub>L<sup>3</sup>]**, **6**. (0.271 g, 80%); white solid. Anal. Calcd for  $\text{C}_{27}\text{H}_{33}\text{N}_2\text{O}_8\text{Tb}$ : C, 48.22; H, 4.95; N, 4.17. Found: C, 47.81; H, 4.81; N, 4.15. mp 261 °C.

**[Er(acac)<sub>3</sub>L<sup>3</sup>]**, **7**. (0.275 g, 82%); white solid. Anal. Calcd for  $\text{C}_{27}\text{H}_{33}\text{N}_2\text{O}_8\text{Er}$ : C, 47.63; H, 4.89; N, 4.11. Found: C, 47.36; H, 4.92; N, 4.52. mp 260 °C.

**[Yb(acac)<sub>3</sub>L<sup>3</sup>]**, **8**. (0.213 g, 63%); white solid. Anal. Calcd for  $\text{C}_{27}\text{H}_{33}\text{N}_2\text{O}_8\text{Yb}$ : C, 47.23; H, 4.84; N, 4.08. Found: C, 46.98; H, 4.74; N, 4.11. mp 258 °C.

**[Eu(acac)<sub>3</sub>L<sup>4</sup>]**, **9**. (0.140 g, 69%); brown solid. Anal. Calcd for  $\text{C}_{43}\text{H}_{61}\text{N}_2\text{O}_8\text{Eu}$ : C, 58.30; H, 6.94; N, 3.16. Found: C, 57.91; H, 6.93; N, 2.91. Thermal behavior: C 67.5 °C, C' 177.7 °C, CL 180.3 °C I.

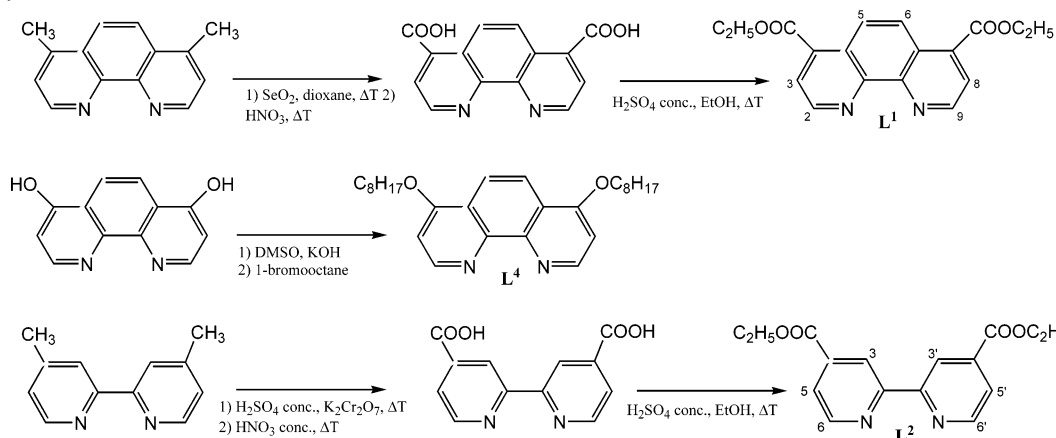
**Crystallography.** Details of the crystal data collection are listed in Table 1. X-ray data for **1** were collected on a Siemens R3m/V automated four-circle diffractometer equipped with graphite-monochromated Mo K $\alpha$  radiation ( $\lambda = 0.71073$ ). The data were corrected for Lorentz and polarization effects. An empirical absorption correction was applied using a method based upon azimuthal ( $\Psi$ ) scan data. X-ray data for **7** were collected on a Bruker-Nonius X8 Apex CCD area detector equipped with graphite monochromator and Mo K $\alpha$  radiation ( $\lambda = 0.71073$ ), and data reduction was performed using the SAINT programs; absorption corrections based on multiscan were obtained by SADABS.<sup>25</sup> Both structures were solved by Patterson method (SHELXS/L program in the SHELXTL-NT software package)<sup>26</sup> and refined by full-matrix least-squares based on *F*<sup>2</sup>. All non-hydrogen atoms were refined anisotropically (with the exception of the methyl carbon atom C(21) of one acac disordered molecule in **7**), and hydrogen atoms were included as idealized atoms riding on the respective carbon atoms with C–H bond lengths appropriate to the carbon atom hybridization. The crystal structure of **7** was solved in the noncentrosymmetric *P2<sub>1</sub>* space group, and the *x* Flack parameter was refined using the racemic twinning routine. In **7**, one of the methyl carbon atoms of

(25) SMART, SAINT, and SADABS; Bruker AXS, Inc.: Madison, WI, 1997.

(26) SHELXTL-NT Crystal Structure Analysis Package, Version 5.1; Bruker AXS Inc.: Madison, WI, 1999.

## Synthesis of Novel Ln(III) $\beta$ -Diketone Complexes

**Scheme 1.** Synthetic Route to  $L^m$  Ligands



the acac ligands was found to be disordered in two positions, both included in the refinement.

**Photophysical Measurements.** Solvents used for the photophysical investigations were spectrofluorimetric grade (Acros Organics). Absorption spectra were recorded with a Perkin-Elmer Lambda 900 spectrophotometer. Corrected emission and excitation spectra were obtained with a Perkin-Elmer LS-50B spectrofluorimeter. Fluorescence quantum yields were measured with the method described by Demas and Crosby<sup>27</sup> using as standard [Ru-(bipy)<sub>3</sub>]Cl<sub>2</sub> (bipy = 2,2'-bipyridine;  $\Phi = 0.028$  in air-equilibrated water<sup>28</sup>) and integrating the emission from 460 to 650 nm for the Tb complexes, and from 550 to 750 nm for the Eu complex, while the excitation wavelength was fixed at 280 nm; all solutions were isoabsorbent with the standard at 280 nm, with  $A < 0.2$ , and cutoff filters were employed to avoid that excitation light impacts the detector. The experimental uncertainty in the band maximum for absorption and luminescence spectra is 2 nm; that for luminescence intensity is 10%.

## Results and Discussion

**Synthesis.** The synthetic pathway to the 4,7-disubstituted 1,10-phenanthroline ligands  $L^1$  and  $L^4$  is outlined in Scheme 1. The 4,7-dimethyl-1,10-phenanthroline was converted, in three steps, to the corresponding acid, whose reaction with sulfurous acid in ethanol afforded the diester  $L^1$ .

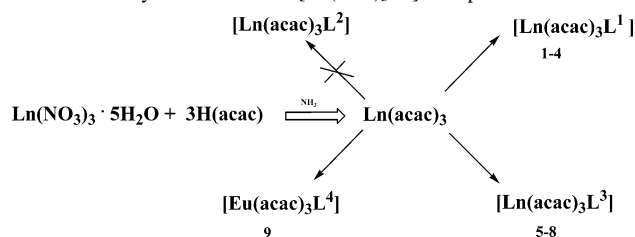
4,7-Dioctyloxy-1,10-phenanthroline,  $L^4$ , was obtained directly by etherification of 4,7-dihydroxy-1,10-phenanthroline with 1-bromooctane, in DMSO and KOH.

For the synthesis of the bipyridine ligand  $L^2$ , the first step, oxidation of the 4,4'-dimethyl-2,2'-bipyridine with potassium dichromate, afforded the diacid, which was converted into the diester  $L^2$  under acid-catalyzed conditions.

Complexes **1–9** were prepared according to Scheme 2.

Complexes **1–4** were prepared by stirring equimolar amounts of the diethyl 1,10-phenanthroline-4,7-dicarboxylate,  $L^1$ , and the appropriate lanthanide acetylacetonate, synthesized according to the literature method, at room temperature, in toluene, for 15 days. However, attempts to prepare the analogues lanthanide complexes of the diethyl 2,2'-bipyridine-4,4'-dicarboxylate under similar conditions were unfruitful, and the unreacted ligand was always recovered. This

**Scheme 2.** Synthetic Route to [Ln(acac)<sub>3</sub>L<sup>m</sup>] Complexes



behavior accounts for an electronic destabilization of the esteric groups on the aromatic bipyridine core, which, associated with a more flexible conformation with respect to the phenanthroline, makes this ligand not compatible with the chelation of a lanthanide ion of any size.

To check for the influence of the substituents on the basicity and the coordination ability of the N,N aromatic ligands, the  $L^3$  bipyridine, bearing a methoxy group in 4,4' position, was used: the activation toward coordination was dramatically enhanced, and complexes **5–8** were isolated in very high yields.

This latter route was followed to explore the electronic as well as the thermal properties of the europium derivative of an opportunely designed promesogenic phenanthroline. Complex **9** was successfully prepared by reaction with  $L^4$ , bearing long ether substituents, and a promesogenic species was obtained. The evidence of the existence of a mesophase has been detected by differential scanning calorimetry (DSC) analysis, the trace of which showed an overlap of the clearing and the melting peaks in a very narrow range of temperature (see Supporting Information). The observation through polarizing optical microscopy, although showing a well-defined texture (see Supporting Information), was not enough to identify the symmetry of the mesophase observed over a few degrees before the clearing point. In any case, it is interesting to point out how it is possible to induce mesomorphism in these systems, generating a promesogenic structure, judiciously functionalizing the phenanthroline ligand in  $p,p'$ -positions with respect to the nitrogen atoms.

**Structural Investigation by X-ray and CSD Database Analysis.** Drawings of complexes [Eu(acac)<sub>3</sub>L<sup>1</sup>], **1**, and [Er(acac)<sub>3</sub>L<sup>3</sup>], **7**, with the selected atom-labeling scheme are shown in Figures 1 and 2; the relevant bond lengths and angles are listed in Table 2.

(27) Demas, J. N.; Crosby, G. A. *J. Phys. Chem.* **1971**, *75*, 991–1024.

(28) Nakamaru, K. *Bull. Chem. Soc. Jpn.* **1982**, *55*, 2697–2705.

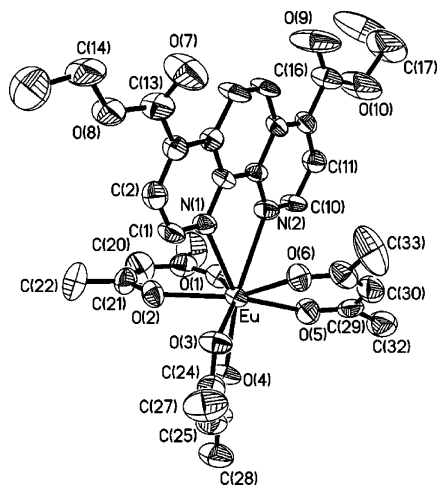


**Figure 1.** Perspective view of the complex **1** with atomic numbering scheme (ellipsoids at the 50% level). Hydrogen atoms are omitted for clarity.

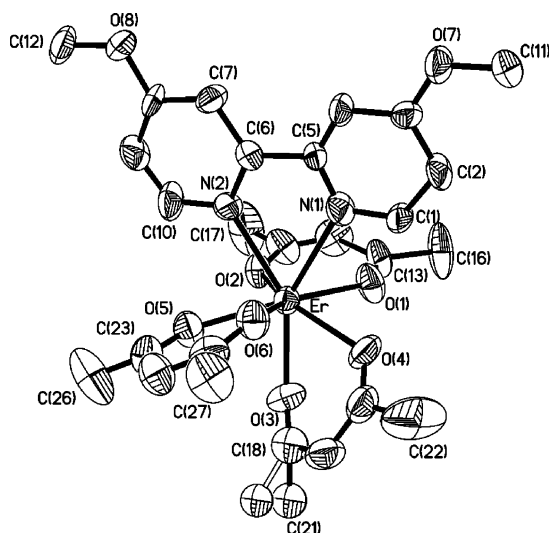


**Figure 2.** Perspective view of the complex **7** with atomic numbering scheme (ellipsoids at the 50% level). Hydrogen atoms are omitted for clarity.

**Table 2.** Selected Bond Lengths (Å) and Angles (deg) for Complexes **1** and **7**

	<b>1</b>	<b>7</b>
Ln–O(1)	2.362(6)	2.317(9)
Ln–O(2)	2.376(6)	2.326(9)
Ln–O(3)	2.368(7)	2.315(3)
Ln–O(4)	2.349(6)	2.347(9)
Ln–O(5)	2.354(7)	2.307(9)
Ln–O(6)	2.354(7)	2.310(3)
Ln–N(1)	2.655(7)	2.612(10)
Ln–N(2)	2.683(7)	2.484(9)
O(1)–Ln–O(2)	72.8(2)	73.7(1)
O(3)–Ln–O(4)	73.1(2)	73.2(4)
O(5)–Ln–O(6)	72.4(2)	74.1(4)
N(1)–Ln–N(2)	60.4(2)	62.0(1)

The structures consist of  $[\text{Ln}(\text{acac})_3\text{L}^m]$  molecules in which each metal ion is octa-coordinated by six oxygen atoms of the three bidentate acetylacetonate ligands and two nitrogen atoms of a bidentate N,N aromatic ligand. These atoms lie at the apexes of a slightly distorted square antiprism, the O-face formed exclusively by oxygen atoms [O(3), O(4), O(5), and O(6)] and the N,O-face formed by two nitrogen atoms and two oxygen atoms [N(1), N(2), O(1), and O(2)].

The square faces are almost parallel as shown by the dihedral angles between the two mean planes:  $2.0(3)^\circ$  in **1** and  $2.1(2)^\circ$  in **7**. The antiprismatic arrangement is common among rare earth metal complexes, and, as in the analogous Ln(III) acetylacetonate phenanthroline derivatives, the ligands span the opposite edges of the two square faces of the coordination antiprism (*s* edges).<sup>14,20</sup>

The average bond lengths and angles of the acetylacetonate ligands are similar to those reported for other acetylacetonate complexes.<sup>14,15,20</sup> The Ln–O bonds in both cases are not affected by the electronic effects that the substituent on the N,N aromatic ligands may exert. The presence of two carboxyethyl groups on the 4,7 positions of the phenanthroline ligand in **1** has a certain effect on the Eu–N bond distances (average  $2.67 \text{ \AA}$ ) and on the bite angle ( $60.4(2)^\circ$ ), the former being slightly longer than those found in the analogues tris-acetylacetonate nonsubstituted phenanthroline derivatives.<sup>20,29</sup>

Plotting the average Ln–N bond distances against the N–Ln–N angles found performing the CSD<sup>30</sup> search for the fragment  $[\text{Ln}^{\text{III}}(\text{phen})]$  (Figure 3a), it appeared quite clear that (i) the Ln–N bond distances are somehow influenced by the nature and the environment around the metal ion in the absence of *p,p'* substituents on the phenanthroline ligands (for instance, the steric and electronic effects of the other ligands around the metal ions) and (ii) the Ln–N bond distances are negatively correlated to the “bite” angle of the phenanthroline ligand. In the case of complex **1**, the presence of two electron-attracting groups in *para*-positions with respect to the nitrogen coordinating atoms causes a lengthening of the bond distances between the Eu(III) ion and the neutral N,N aromatic ligand. In fact, the “ $\Delta$ ” in Figure 3a corresponding to complex **1** is well out of the cluster of points relative to the crystal structures containing Eu(III) found in the search (“ $\times$ ”).

In the case of complex **7**, the average Er–N bond distance,  $2.55 \text{ \AA}$ , is found to be slightly longer than expected from the size of the lanthanide ion and the flexibility of the bipyridine ligand. Even if a direct comparison with tris-acetylacetonate erbium(III) complexes containing nonsubstituted bipyridines is not possible due to the lack of crystal structures in the literature, there are other examples of tris-chelate bipyridine Er(III) derivatives for which the average Er–N bond distances are found to be slightly shorter than that found in **7**.<sup>31</sup> If the crystal structure of **7** is included in the CSD search for the fragment  $[\text{Ln}^{\text{III}}(\text{bipy})]$  (point marked “ $\Delta$ ”), it is possible to note that the data relative to complex **7** is just out of the cluster points containing the Er(III) structures (Figure 3b).

(29) Ahmed, M. O.; Liao, J.-L.; Chen, X.; Chen, S.-A.; Kaldis, J. H. *Acta Crystallogr., Sect. E* **2003**, *59*, m29.

(30) The search of the Cambridge Structural Database (Version 5.25) was conducted on the generic fragments  $[\text{Ln}^{\text{III}}(\text{phen})]$  and  $[\text{Ln}^{\text{III}}(\text{bipy})]$  found in crystal structures containing lanthanide ions in coordination numbers 8, 9, and 10, and was restricted to ordered and error-free structures (*R* factor < 0.1). While in the case of the fragment  $[\text{Ln}^{\text{III}}(\text{phen})]$  only crystal structures of nonsubstituted phenanthroline complexes have been found, in the case of  $[\text{Ln}^{\text{III}}(\text{bipy})]$  one structure containing the ligand 4,4'-dimethyl-2,2'-bipyridine is included in the analysis.

(31) Su, C.; Tang, N.; Tan, M.; Yu, K. *Polyhedron* **1996**, *15*, 233–239.

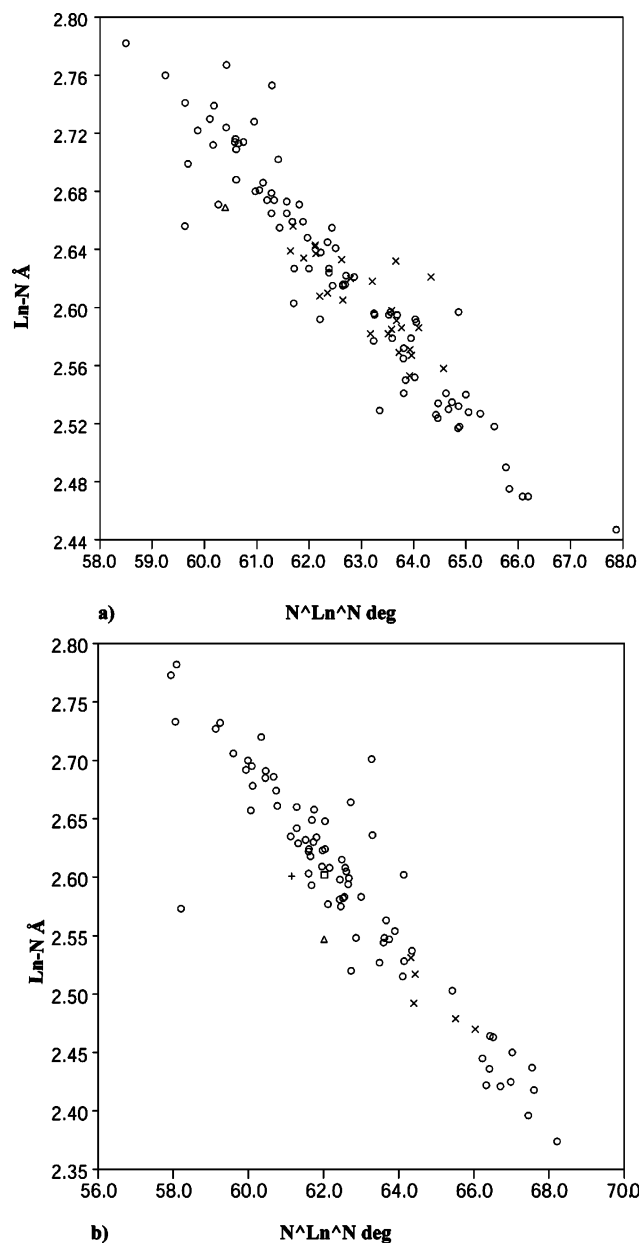


**Figure 3.** The average bond distance Ln–N plotted against the bond angle  $N^{\wedge}Ln^{\wedge}N$  for fragments  $[Ln(phen)]$  (a), where the sign “ $\times$ ” denotes structures containing Eu(III), and  $[Ln(bipy)]$  (b), where the sign “ $\times$ ” denotes structures containing Er(III).

Considering the moderately electron-donating nature of the two substituents on the bipyridine in **7**, which should contribute to an increase in the interaction between the cation and the corresponding ligand,<sup>32</sup> the slight lengthening of the Er–N bond distances could only be attributable to structural effects instead of electronic ones. The presence of *p,p'* substituents on the bipyridine does not allow the ligand (which is in a N,N-trans conformation when not coordinated) to adopt an optimal coordination mode for the N,N binding site approaching the Er(acac)<sub>3</sub> substrate, with the effect of perturbing the Er–N bond distances. The same effect is also observed in the case of two Eu(III) dibenzoylmethanate derivatives (Refcodes in CSD search majzom and lelup, see

(32) Berny, F.; Muzet, N.; Troxler, L.; Dedieu, A.; Wipff, G. *Inorg. Chem.* **1999**, *38*, 1244–1252.

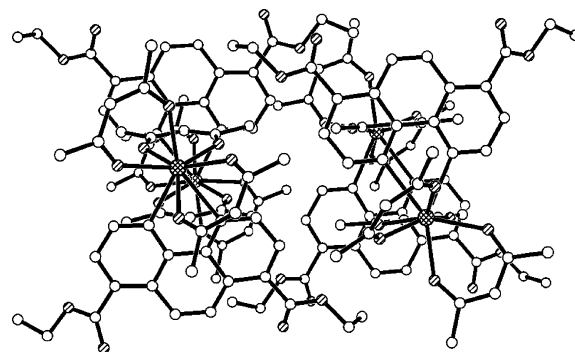


**Figure 4.** Ball-and-stick representation of the association of hemi-disk-like molecules of complex **1** viewed down the *b* axis.

**Table 3.** Photophysical Parameters in Methanol Solution

compound	abs, $\lambda/nm(\epsilon/M^{-1} cm^{-1})$	em, $\lambda/nm$	$\Phi$
L <sup>1</sup>	290(24 630)	420	0.030
L <sup>3</sup>	258(11 230), 274(9680)	360	0.040
[Tb(acac) <sub>3</sub> L <sup>1</sup> ], <b>2</b>	284(46 100)	492, 546, 587, 620, 646	0.006
[Eu(acac) <sub>3</sub> L <sup>3</sup> ], <b>5</b>	275(35 100), 310(sh)	580, 592, 615, 651, 700	$1.2 \times 10^{-4}$
[Tb(acac) <sub>3</sub> L <sup>3</sup> ], <b>6</b>	280(33 630)	492, 546, 587, 620, 646	0.043

Supporting Information). The presence of two methyl groups on the bipyridine (crystal structure marked “+” in Figure 3b) causes a slight difference in the interaction between the ligand and the lanthanide ion when compared to the analogous complex with a nonsubstituted bipyridine (point marked “ $\square$ ”) as evidenced by a smaller bite angle.

In 3D space, molecules of complex **1** are found to be stacked along the *b* direction with a Eu–Eu distance 8.7 Å caused by the presence of acetylacetonate ligands between the two molecules (Figure 4). The coplanar phenanthroline ligands of the two molecules span from opposite sides generating layers of aromatic rings joined together through alkoxy interdigitated chains and separated by the Eu(acac)<sub>3</sub> core of the molecules.

**Optical Spectroscopy.** UV–vis spectroscopic data obtained in methanol at room temperature for complexes **2**, **5**, **6**, and their ligands are presented in Table 3. Unfortunately, complexes **1** and **9** were unstable under the experimental conditions, losing the N, N aromatic ligand in solution. The Er(III) and Yb(III) complexes **3**, **4**, **7**, and **8** showed nonsensitized emission in the 400–700 nm range.

Absorption spectra of the compounds **2**, **5**, and **6** are reported in Figure 5; the comparison shows that the spectral features of these complexes are due to their aromatic ligands, taking into account a slight blue-shift due to the perturbation induced by the metal coordination.

For complex **2**, excitation corresponding to the intense ligand absorption band at 284 nm results in sensitization of the metal-centered luminescence; a similar spectral pattern is obtained by exciting the absorption maximum of complex **6** (Figure 6).

The light absorption of the aromatic ligand, which acts as an antenna system, produces an excited, ligand-localized, singlet state, followed by an intersystem crossing to the lowest-lying triplet level, and an energy transfer toward the <sup>5</sup>D<sub>4</sub> excited Tb(III) state. The transitions observed in the 475–700 nm range are due to the deactivation of the <sup>5</sup>D<sub>4</sub>

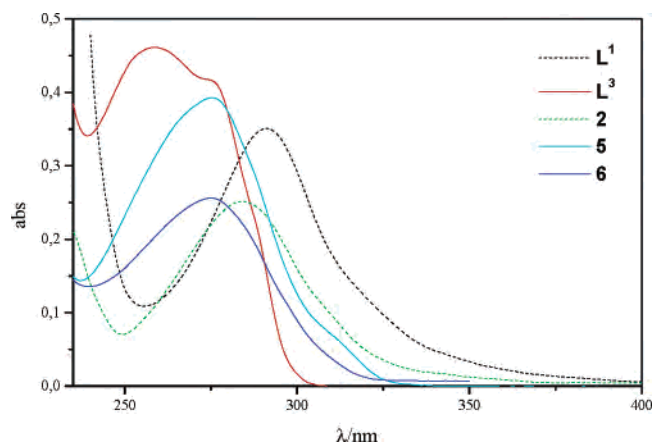


**Figure 5.** Absorption spectra of ligands  $L^1$  and  $L^3$  and complexes **2**, **5**, and **6** collected in methanol solution.

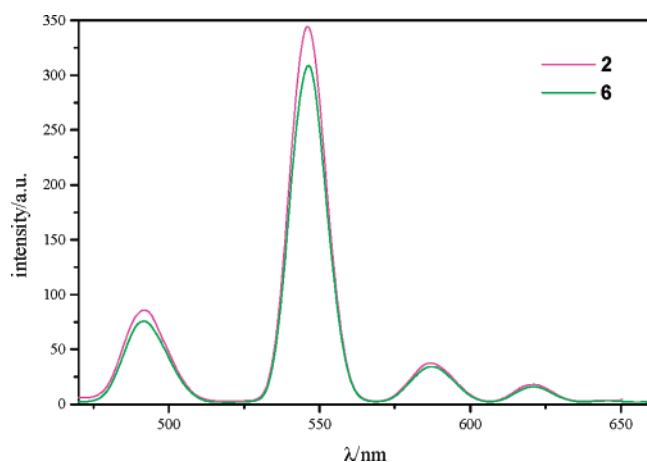


**Figure 6.** Emissions of Tb(III) complexes **2** and **6** in methanol solution; excitation spectra confirmed sensitization of the metal-centered luminescence.

state to the  ${}^7F_J$  ( $J = 2-6$ ) levels. The  ${}^5D_4 \rightarrow {}^7F_4$  transition around 587 nm is sensitive to the coordination,<sup>33</sup> and the overlap of this band in both complexes is indicative of a similar coordination environment. The sensitized emission quantum yield ( $\Phi$ ) obtained for complex **2** is almost 1 order of magnitude lower than the corresponding value in  $L^1$  (Table 3). It is relevant that deactivation of the triplet level by oxygen quenching is not observed; that is, air-equilibrated and argon-bubbled samples yielded the same intensity of luminescence spectra. This insensitivity to oxygen quenching is also observed in other lanthanide complexes and is referred to rapid energy transfer toward the ion center ( $<20$  ns), probably from the antenna singlet state.<sup>34</sup> Furthermore, no difference was found in the dichloromethane solution luminescence spectrum, thus demonstrating that no relevant quenching of emission is due to the vibronic coupling with O–H oscillators. The loss in radiative deactivation observed in **2** can be ascribed to a back-energy transfer between the metal emitting-state and the lowest-excited state of the ligand.<sup>35</sup> On the contrary, no loss of luminescence intensity

(33) *Lanthanide Probes in Life, Chemical and Earth Science*; Bünzli, J.-C. G., Choppin, G. R., Eds.; Elsevier: Amsterdam, 1989.

(34) van der Tol, E. B.; van Ramesdonk, H. J.; Verhoeven, J. W.; Steemers, F. J.; Kerver, E. G.; Verboom, W.; Reinhoudt, D. N. *Chem.-Eur. J.* **1998**, *4*, 2315–2323.

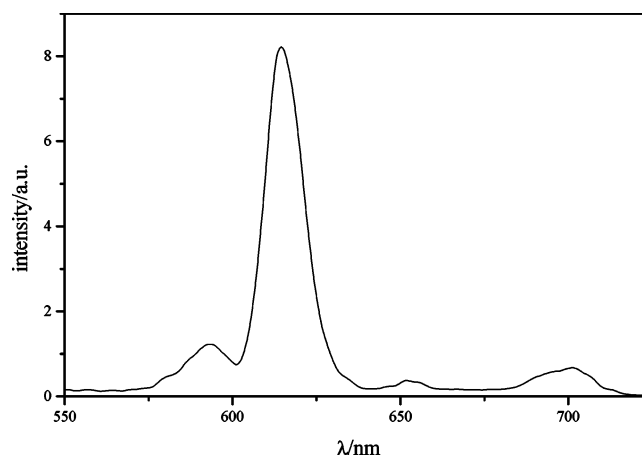


**Figure 7.** Emission spectrum of complex **5** in methanol solution.

is observed in the case of complex **6**, the emission quantum yield of which is almost the same as its ligand  $L^3$ . In fact, if one compares the emission maximum of this ligand (Table 3) with that of  $L^1$  (whose position is related to that of the triplet transferring state), it can be noted that the  $L^3$  emitting state is higher in energy, thus preventing the back-energy transfer. In this way, the sensitization of the metal-centered luminescence in **6** is about complete. In both cases, the observed reduction of the quantum yield when compared with similar ternary acetylacetonate complexes is caused by the introduction of the neutral aromatic ligands, as already reported for analogous systems.<sup>36</sup>

The europium complex **5** shows a series of emission peaks in the 575–725 nm region (Figure 7); these are transitions from the  ${}^5D_0$  excited state to the  ${}^7F_J$  ( $J = 0-4$ ) levels. The most intense transition in the emission spectrum is the  ${}^5D_0 \rightarrow {}^7F_2$  transition at 615 nm; this is the so-called hypersensitive transition and is responsible for the brilliant red emission color of this complex.<sup>37</sup> The luminescent quantum yield is 2 orders of magnitude lower than  $L^3$  and the homologous terbium complex **6**; because slight differences in  $\Phi$ -values were detected between air-equilibrated and argon-bubbled samples, and between methanol and anhydrous dichloromethane solution, the relevant emission quenching is ascribed to the presence of a ligand-to-metal charge-transfer (LMCT) state, which can be deactivated via a nonradiative path. In fact, it is well known<sup>33</sup> that europium complexes have LMCT states at low energy, because the Eu(III) ion is easily reduced ( $E^\circ$  (Eu(III)/Eu(II)) =  $-0.38$  V).

## Conclusions

In the present study, we have investigated the influence of different substituents in  $p,p'$ -positions, with respect to the nitrogen atoms in phenanthroline and bipyridine ligands, on

(35) Latva, M.; Takalo, H.; Mikkala, V.-M.; Matachescu, C.; Rodriguez-Ubis, J. C.; Kankare, J. *J. Lumin.* **1997**, *75*, 149–169.

(36) Voloshin, A. I.; Shavaleev, N. M.; Kazakov, V. P. *J. Photochem. Photobiol., A* **2000**, *136*, 203–208.

(37) Sabbatini, N.; Guardigli, M.; Manet, I. Antenna Effect in Encapsulation Complexes of Lanthanide Ions. In *Handbook on the Physics and Chemistry of Rare Earth*; Gschneider, K. A., Jr., Eyring, L., Eds.; Elsevier Science B. V.: New York, 1996; pp 69–119.

the coordination capability and on the physical properties of several complexes of the general formula  $[\text{Ln}(\text{acac})_3\text{L}^m]$ . The electronic effects exerted by the substituents on the basicity of the nitrogen atoms are dramatic in the case of the bipyridine systems. In fact, with electron-attracting groups, such as in **L**<sup>2</sup>, no coordination to any lanthanide ions was observed. An enhanced basicity of the coordinating nitrogen atoms was detected by replacing the substituents with two electron-donating groups (OCH<sub>3</sub> in **L**<sup>3</sup>), and in this case complexes **5–8** were isolated and **7** was structurally characterized. The analysis of the Ln–N bond distances in the solid state of lanthanide bipyridine complexes, as compared to those found in complex **7**, has pointed out that in the coordination of bipyridines to Ln(III) ions there is a balance between electronic and structural effects which depends both on the nature and the presence of substituents in the *p,p'*-position with respect to the nitrogen atoms. In fact, the average Er–N bond distance (2.55 Å) in **7** is found to be slightly longer than expected from the size of the Er(III) ion and the presence of electron-donating groups on the bipyridine ligand, indicating that this ligand may not adopt an optimal coordination mode when approaching the Ln cation already surrounded by other coordinants, with a consequent perturbation of the Ln–N bond distances.

On the other hand, the presence of two carboxyethyl groups on the 4,7 positions of the phenanthroline ligand **L**<sup>1</sup> does not prevent coordination to these Ln(III) ions, and the only effect observed in the synthesized complex **1**, whose single-crystal structure is reported here, is a certain lengthening of the Eu–N bond distances with respect to those found for Ln complexes containing phenanthroline, which is not disubstituted. These results are in agreement with those reported from a quantum mechanics study on the interaction energy between lanthanide cations and N aromatic ligands bearing groups with different electronic properties in the *para*-position.<sup>32</sup>

The lengthening of the Eu–N bond distances observed in the solid state became a strong instability once in solution. In fact, the loss of the aromatic ligand was detected by performing UV–vis spectroscopic analysis, and therefore no results were obtained concerning absorption and emission

properties of **1**. Although the increased basicity of the phenanthroline ligand, obtained by replacing the two carboxyethyl groups with two alkoxy substituents (**L**<sup>4</sup>), should induce a stronger chelation of the Eu(III) ion, complex **9** showed only slightly improved stability in solution. In fact, in this case, the loss of the ligand is a slow process, and in the emission spectra recorded in solution it is possible to observe the decrease of the sensitized emission while the ligand emission increases during the collection of the spectrum; thus, no measurement of the emission quantum yield was performed on this complex. On the other hand, a slight change in size (and hence in hardness) of the Ln(III) ion (moving from Eu(III) to Tb(III)) produced an increase in stability such that it was possible to perform the UV–vis spectroscopic analysis in solution in the case of the Tb(III) **L**<sup>1</sup> derivative (complex **2**) and observe the expected metal-centered luminescence. Concerning the bipyridine **L**<sup>3</sup> lanthanide derivatives, while the Er(III) and Yb(III) complexes (**7** and **8**) showed no sensitized emission in the UV–vis range, the Eu(III) and Tb(III) derivatives (**5** and **6**) performed an appreciable energy transfer from the ligand to the metal. In particular, complex **6** showed a complete transfer, and the emission quantum yield is almost the same as its ligand **L**<sup>3</sup>.

Moreover, the use of relatively long alkoxy chains as substituents on the 1,10-phenanthroline ligand (**L**<sup>4</sup>) led to the formation of the promesogenic Eu(III) complex, **9**, whose thermal behavior is encouraging for the synthesis of new lanthanide liquid-crystalline species.

**Acknowledgment.** This work was partly supported by the Ministero dell'Istruzione, dell'Università e della Ricerca through the Centro di Eccellenza CEMIF.CAL grant.

**Supporting Information Available:** Listings of the photo micrograph of the texture and DSC thermogram of complex **9**, refcodes, and geometrical parameters of the crystal structures included in the CSD search. Crystallographic data in CIF format. This material is available free of charge via the Internet at <http://pubs.acs.org>.

IC048951R